Interfacial Chemistry

Deutsche Ausgabe: DOI: 10.1002/ange.201502069
Internationale Ausgabe: DOI: 10.1002/anie.201502069

Tuning the Metal–Support Interaction by Structural Recognition of Cobalt-Based Catalyst Precursors**

Kim Larmier, Céline Chizallet, and Pascal Raybaud*

Abstract: *Controlling the nature and size of cobalt(II) polynuclear precursors on γ-alumina and silica-alumina supports represents a challenge for the synthesis of optimal cobalt-based heterogeneous catalysts. By density functional theory (DFT) calculations, we show how after drying the interaction of cobalt(II) precursor on γ-alumina is driven by a structural recognition phenomenon, leading to the formation of an epitaxial $Co(OH)_2$ precipitate involving a Co–Al hydrotalcite-like interface. On a silica-alumina surface, this phenomenon is prevented due to the passivation effect of silica domains. This finding opens new routes to tune the metal–support interaction at the synthesis step of heterogeneous catalysts.*

Controlling the phenomena occurring at the interface between oxidic materials and metallic complexes has been a challenging topic during the last decades.[1] Indeed, they are involved in several environmentally and industrially important situations, such as corrosion, water treatments, and catalyst preparation. Cobalt in particular has drawn much attention: ^{60}Co is a radioactive isotope found in nuclear process wastewaters, whereas cobalt-containing heterogeneous catalysts are widely used for hydrodesulfurization reactions,[2] Fischer–Tropsch synthesis[3] (both examples enabling the production of cleaner fuels), oxygen evolution reactions,[4] and a large set of C_1 chemistry reactions (CO oxidation,[5] dry reforming of methane,[6] inter alia). γ-alumina[7] or amorphous silica-alumina[8] are used industrially as efficient Co sorbent or supports for such applications.[9] Cobalt (as well as nickel) is known to exhibit strong chemical interactions with the γ-alumina surface at the various preparation steps of catalysts (impregnation, drying, and/or calcination) which may lead to the formation of hardly reducible hydroxides or even mixed aluminium–cobalt (nickel) oxide phases being detrimental to the final catalytic activity.[1d,9,10] This feature might be explained by the adsorption mode and strength of cobalt precursors on the γ-alumina surface. Although UV-visible spectroscopy[10d,11] and EXAFS[1e,12] analyses brought insights on the local environment of adsorbed Co species, the chemical nature and local structure of the interface between cobalt species and the surface remain to be unraveled, which is mandatory for the control of the final catalyst. DFT calculations have shown their ability to provide predictive molecular insight in the structure of complex catalytic systems, including supported transition metals.[13]

Herein, we propose a DFT study of the interaction of the most widely used cobalt precursor, cobalt(II) hexahydrate ($Co(H_2O)_6^{2+}$), with the γ-alumina surface as predominant after the drying step of the preparation process. We reveal a specific interaction between the cobalt precursor and the surface, different from the simple OH exchange usually invoked[14] and consistent with the concept of structural recognition, developed in the field of biochemistry by E. Fischer,[15] extended to chemistry and supramolecular chemistry,[16] and later by M. Che et al. to interfacial chemistry for the interaction of metallic complexes with inorganic surfaces.[17] We then propose a thermodynamic mechanism for the growth of Co-hydroxide over γ-alumina occurring during deposition. Lastly, we predict that structural recognition is prevented on a silica-alumina surface, which impacts the nature of cobalt species at the surface.

The adsorption of a cobalt(II) precursor was first investigated on the (100) and (110) γ-alumina surface, with models developed by Digne et al.[18] (Supporting Information (SI) S1). To mimic the residual interactions of the cobalt precursor with the alumina surfaces after a mild drying at room temperature, both surfaces were considered in their highest hydration state (about 17 $OH\,nm^{-2}$ each, under $P(H_2O) = 1$ bar). The Gibbs free energy of cobalt monomer adsorption $\Delta_r G°_{ads}$ was quantified at 298 K (SI S2) to allow a consistent comparison with previous experimental data.[1e,13] General trends hold true for higher drying temperature (up to ≈400 K) as used in many other experiments[9,10d,11] (SI S5). In a first step, a suitable octahedral inner-sphere mononuclear complex was examined at low Co coverage (0.37 and 0.53 $Co\,nm^{-2}$ on the (110) and (100) surface, respectively), following insights from UV-visible spectroscopy[11] and EXAFS.[1e,12] Several coordination modes and surface sites were investigated (SI S3): the most relevant configurations are reported in Figure 1. Any attempt to produce a mono- or bidentate octahedral inner-sphere complex bound only to surface hydroxy groups (μ_1-OH, Scheme 1) proved unsuccessful, and led to tetrahedral-like species (Figure 1c), with spontaneous removal of two water molecules from the coordination sphere of cobalt during optimization. Such systems were characterized by $\Delta_r G°_{ads} = -174\ kJ\,mol^{-1}$ for the most stable one. Thus, we investigated other possible surface coordination modes involving alumina oxygen atoms. On both (100) and (110) surfaces, it was possible to identify much more favorable octahedral structures (Figure 1a,b),

[*] K. Larmier, Dr. C. Chizallet, Dr. P. Raybaud
IFP Energies nouvelles
BP3, 69360 Solaize (France)
E-mail: celine.chizallet@ifpen.fr

[**] The authors thank V. Lecoq and F. Diehl (IFP Energies nouvelles), and E. Marceau (UPMC—Paris) for fruitful discussions. Part of this work was supported by the French National Research Agency within the framework of the ANR-14-CE08-0019 SLIMCAT project.

Supporting information for this article is available on the WWW under http://dx.doi.org/10.1002/anie.201502069.

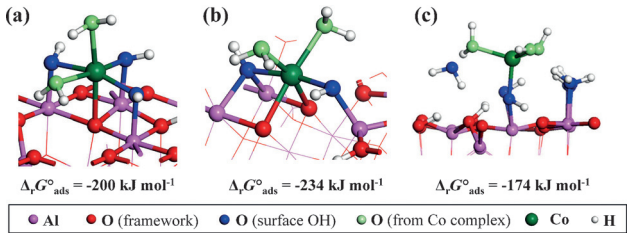

Figure 1. Optimized structures of: most stable octahedral inner-sphere complexes on the a) (100) surface, b) (110) surface. c) Tetrahedral complex as obtained by exchange with μ_1-OH ligands only.

Table 1: Interatomic distances (in Å) in several oxidic materials and in our models of cobalt precursor adsorbed on alumina described above.

Material	Co–O	Co–Al	Co–Co	Reference
β-Co(OH)$_2$	2.10	–	3.17	[1e]
Co-Al hydrotalcite	2.08	3.08	–	[1d]
Co/γ-alumina	2.08	3.27	3.14	[1e]
Co/γ-alumina (100)[a]	2.13	3.02	3.08	this work
Co/γ-alumina (110)[a]	2.13	3.10	2.80–2.89	this work
Co/kaolin	2.08	3.25	3.14	[1e]
Co/ASA[a]	2.11	3.06	–	this work

[a] For the most stable configuration for each Co coverage (from 0.37 to 2.22 nm^{-2}).

with Co–O and Co–Al distances consistent with EXAFS[1e,12] (Table 1). The octahedral coordination sphere of the cobalt atom involved three types of oxygen atoms:

- One or two oxygen atoms (red) initially of μ_2 or μ_3 types and belonging to the alumina framework,
- Three or two (respectively) oxygen atoms from initially μ_1-OH hydroxy groups (dark blue) of the hydration layer and/or of the precursor complex,
- Oxygen atoms (light green) of water molecules from the precursor.

$\Delta_r G°_{ads}$ values are −200 and −234 kJ mol^{-1} on the (100) and (110) surface, respectively. Ab initio molecular dynamics confirm these stable conformations. They are chemically relevant because the cobalt atom is inserted in an octahedral aluminum vacancy created by the cleavage of the surface, and the interaction can be interpreted as a surface structural recognition phenomenon (Scheme 1). This is also expected at edges of alumina particles, as the geometry requirements will be the same. This feature can be understood by comparing the cobalt environment in our models and in reference materials, as β-Co(OH)$_2$ and Co–Al hydrotalcite (Table 1). Co–O and Co–Al distances are rather similar, in particular on (100).

Co coverage was then increased from 0.37 to 2.22 Co nm^{-2}, on the (110) surface (for (100) see SI S5). For two cobalt atoms in the surface cell (0.74 Co nm^{-2}), different configurations were tested: 1) two isolated surface complexes apart from each other ("dispersed", Scheme 1 g); 2) two octahedral surface complexes bound by an edge ("epitaxial", Scheme 1 h); 3) one grafted complex and the second being grafted on top of the first one by an edge, and without direct interaction with the surface ("apical", Scheme 1 i) When a polynuclear species "epitaxial" or "apical" is involved, the local structure exhibits an edge-bound octahedral connectivity (corner-bound octahedra are less stable), as also known for β-cobalt hydroxide (SI S4). The "epitaxial" configuration is the most stable ($\Delta_r G°_{ads} = -209$ kJ mol^{-1}), in close competition with the dispersed mode ($\Delta_r G°_{ads} = -208$ kJ mol^{-1}). The apical mode is less stable by 70 kJ mol^{-1}. Co–Co distance in the "epitaxial" dimer is around 2.90 Å, slightly lower than the Co–Co distance in β-Co(OH)$_2$ (3.17 Å).

This difference can be explained by the structural recognition phenomenon: the dimer is constrained by the interaction with the surface, and the Co–Co distance is related to the Al–Al distance on γ-alumina (2.8 Å). The Co–Co distance on (100) is slightly higher (3.08 Å) and matches the experimental reports (Table 1). The contraction of Co–Co bonds as compared to the reference hydroxide also appears in experimental data from EXAFS.[1e] It was indeed proposed

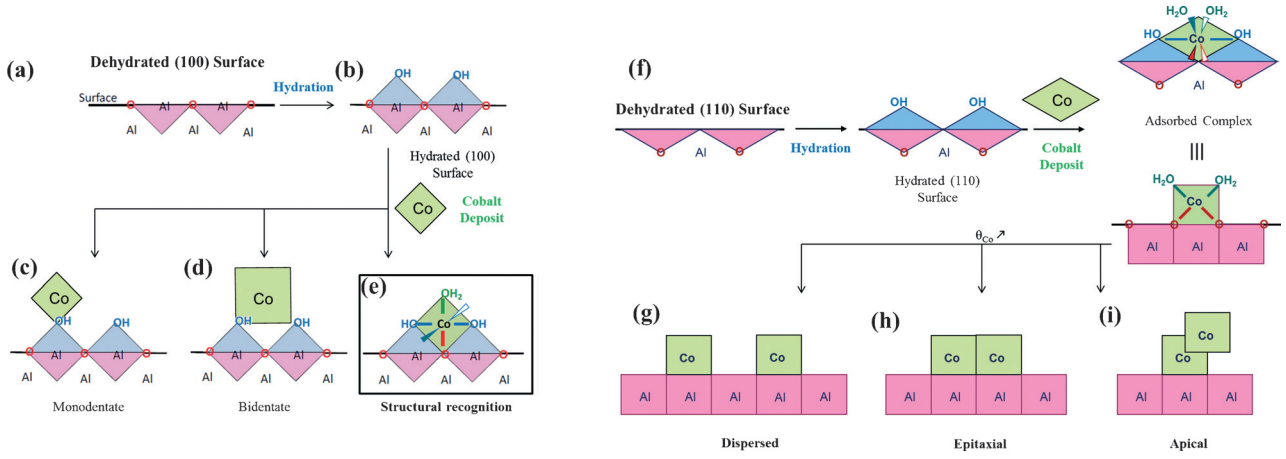

Scheme 1. Polyhedron representation (side view) of surface coordination sphere of Al (pink and blue if ligands are framework O atoms and water O atoms) and Co (green) on γ-alumina. (100) surface: a) dehydrated (mostly Al$_V$ atoms); b) hydrated; expected surface complex according to exchange with μ_1-OH groups: c) monodentate or d) bidentate; e) most favorable mode, implying μ_1-OH and framework oxygen, obtained by structural recognition. (110) surface: f) adsorption of a single Co complex. The right bottom image depicts the Co adsorbed on the (110) surface seen perpendicularly; adsorption of several cobalt complexes: g) dispersed, h) epitaxial, i) apical.

that a "modified $Co(OH)_2$" phase (with contracted dimensions) was grown on the γ-alumina surface.[12] The authors assigned this to possible defects in the hydroxide phase, we propose here that this is due to the epitaxial constraint imposed by the γ-alumina surface. At 1.11 Co nm^{-2} (three Co per unit cell), the dispersed mode appeared to be less stable than the epitaxial mode, which is consistent with EXAFS at the K-edge of adsorbed Co^{II} experiments revealing Co second nearest neighbors far below the monolayer.[1e] The authors concluded the existence of polynuclear species, with a β-hydroxide-like structure (β-$Co(OH)_2$).[12] Our calculation was extended to higher Co coverage on the (110) surface (up to 2.22 Co nm^{-2}, six Co complexes per unit cell). Inspired by the previous results, the connectivity between Co complexes was investigated according to the β-$Co(OH)_2$ structure (Co "epitaxial" oligomers aligned in a single row).

Figure 2 shows the stability of the i^{th} Co-oligomer on the cell containing the most stable surface $(i-1)^{th}$ Co oligomer

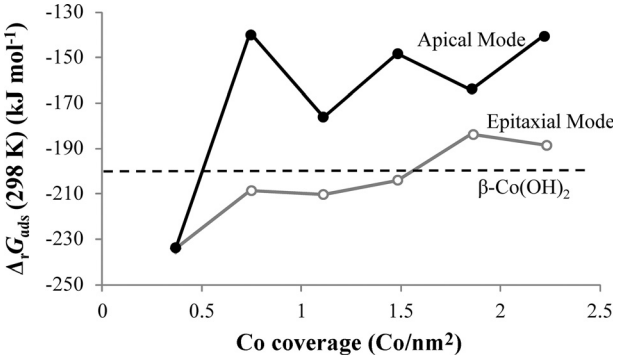

Figure 2. Comparison of $\Delta_r G°_{ads}$ for the apical and epitaxial modes on the (110) surface. The free enthalpy of formation of β-$Co(OH)_2$ from the same Co-initial state is also drawn.

(SI S2), in the "apical" or "epitaxial" mode. At any Co coverage, the "epitaxial" oligomer is favored. At low coverage ($\theta_{Co} < 2$ Co nm^{-2}), $\Delta_r G°_{ads}$ of Co on the γ-alumina (110) surface is lower than the free energy of formation of β-$Co(OH)_2$ from the same initial state (−200 kJ mol^{-1}). This enlightens the stabilizing role of the interaction of surface with cobalt species. At higher Co coverages, this support's stabilizing effect is reduced by the deformed structure of the oligomer with respect to the reference β-$Co(OH)_2$ one. Hence $\Delta_r G°_{ads}$ gets closer to the free energy of formation of β-$Co(OH)_2$. For six atoms in the unit cell ($\theta_{Co} = 2.22$ Co nm^{-2}), an infinite row of Co atoms is bound to the surface, with Peierls-like distortion.

These results allow to propose a thermodynamic mechanism for the growth of the experimentally observed surface cobalt hydroxide, summarized in Scheme 2. First, isolated complexes are grafted following the structural recognition phenomenon evidenced. Beyond ca. 1 Co nm^{-2}, aligned Co oligomers are formed. Above ca. 2 Co nm^{-2}, these rows can initiate the nucleation of Co hydroxide layers as found in the β-hydroxide structure: the Co-complex rows act as anchoring points for the β-$Co(OH)_2$ layers. These layers are constrained to grow on the surface with a tilt angle of about 34° and 60°

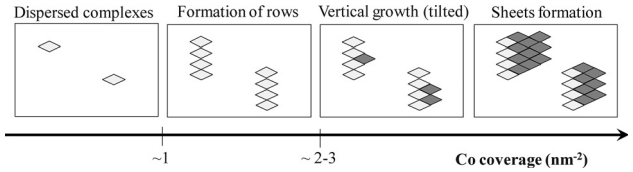

Scheme 2. Mechanism for the growth of β-$Co(OH)_2$ surface precipitate on the γ-alumina surface (top view), according to the thermodynamic stability of plausible intermediates. Light and dark grey polyhedra represent Co complexes grafted to the surface and in the $Co(OH)_2$ sheet, respectively.

and with an interlayer distance of about 4.65 Å and 5.30 Å on the (100) and (110) surface, respectively (SI S7). A similar feature was observed experimentally for the growth of molybdenum oxide on γ-alumina,[19] and recent GI-XAS showed the precipitation pathway of $Ni(OH)_2$ from Ni^{II} species grafted on α-alumina (1–102).[1f] The present work goes beyond: it shows that such a phenomenon can be extrapolated to Co species deposited on an industrial-type γ-alumina support.

Finally, we explored the impact of changing the nature of the surface when a silica overlayer is deposited to form amorphous silica-alumina (ASA), using the model developed by some of us[8,20] (SI S1). This model appears to be relevant for industrial supports, with a high Si coverage of 6.4 Si nm^{-2}.[13b,20] For 0.53 Co nm^{-2}, it was very difficult to isolate a suitable octahedral inner-sphere Co complex. Most of the adsorption free energies (SI S3) were about −140 kJ mol^{-1} for the most stable systems, which is significantly lower than on alumina. We found only one possible configuration in which Co was adsorbed in a pentahedral inner-sphere complex with $\Delta_r G°_{ads} = -207$ kJ mol^{-1} (Figure 3b). The local Co–O and Co–Al distances are comparable

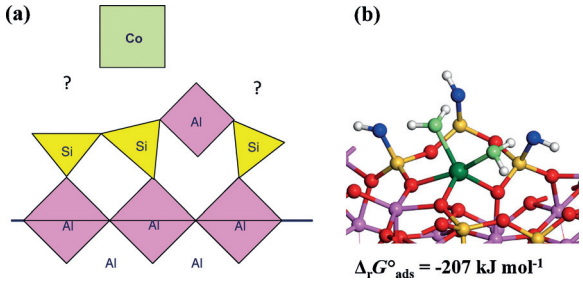

Figure 3. a) Polyhedron representation of the ASA surface (same color code as Scheme 1, and Si coordination sphere in yellow). b) Perspective view of the most stable adsorption configuration found.

with EXAFS (Table 1). However, from this isolated location, it was impossible to construct a row of epitaxial Co oligomer such as on alumina. Hence, the silica overlayer "passivates" the γ-alumina surface and reduces the interaction between the Co complex and the surface. This prevents the formation of a mixed Co–Al oxide phase. Indeed, the structure of the ASA surface is significantly different from that of the γ-alumina: disordered silicon tetrahedra and five-coordinated aluminum, extracted from the alumina surface, appear on the surface (Figure 3a), so that no systematic structural recog-

nition phenomenon can be identified for the cobalt precursor. Experimentally, the high-temperature peak (≈ 800–900 K) of programmed reduction temperature observed of Co species on alumina is not observed on ASA.[9] This is assigned to the absence of epitaxially grown species. As a corollary, we expect that changing the surface Si/Al ratio on ASA will tune the distribution and size of Co oligomers at the silica-alumina surface, which impact the final cobalt catalysts (dispersion, reducibility).[10e,21]

This DFT study provides original insights at the molecular scale on the chemical nature of the interface between a cobalt aqueous precursor and the γ-alumina or silica-alumina surfaces after the drying treatment of the preparation sequence. The tendency for the formation of polynuclear species below the monolayer coverage and a mechanism for the formation of a surface precipitate are proposed on the basis of a structural recognition phenomenon on γ-alumina. These strong epitaxial interactions explain the affinity of cobalt precursors for alumina, which leads to the formation of undesired mixed oxide phases—and the loss of cobalt atoms. Amorphous silica-alumina support (with a high surface Si coverage) prevents this structural recognition phenomenon, due to the presence of a passivating silica overlayer. We hope that this work will pave the way for future DFT simulations devoted to the impregnation step of cobalt on alumina in aqueous medium. More generally, these findings may open perspectives for the optimization at the molecular scale of the synthesis steps of cobalt active phases involved in numerous heterogeneous catalysts.

Methods Section

Periodic DFT calculations were performed by using VASP[22] with the GGA-PBE functional[23] and PAW pseudopotentials.[24] The cut-off energy was equal to 400 eV and the convergence criterion on the forces was fixed at 0.02 eV $Å^{-1}$ for geometry optimizations. Spin-polarized calculations were performed (cobalt(II): d^7 electronic configuration). Additional details about models, thermodynamics, and methods are given in SI S1, S2, and S8.

Keywords: adsorption · catalyst preparation · cobalt · density functional calculations · γ-alumina

How to cite: *Angew. Chem. Int. Ed.* **2015**, *54*, 6824–6827
Angew. Chem. **2015**, *127*, 6928–6931

[1] a) G. E. Brown, V. E. Henrich, W. H. Casey, D. L. Clark, C. Eggleston, A. Felmy, D. W. Goodman, M. Grätzel, G. Maciel, M. I. McCarthy, K. H. Nealson, D. A. Sverjensky, M. F. Toney, J. M. Zachara, *Chem. Rev.* **1999**, *99*, 77; b) K. Bourikas, C. Kordulis, A. Lycourghiotis, *Catal. Rev.* **2006**, *48*, 363–444; c) B. M. Weckhuysen, *Angew. Chem. Int. Ed.* **2009**, *48*, 4910–4943; *Angew. Chem.* **2009**, *121*, 5008–5043; d) J. B. d'Espinose de La Caillerie, M. Kermarec, O. Clause, *J. Am. Chem. Soc.* **1995**, *117*, 11471–11481; e) C. J. Chisholm-Brause, P. A. O'Day, G. E. Brown, G. A. Parks, *Nature* **1990**, *348*, 528–531; f) A. Tougerti, I. Llorens, F. D'Acapito, E. Fonda, J. L. Hazemann, Y. Joly, D. Thiaudiere, M. Che, X. Carrier, *Angew. Chem. Int. Ed.* **2012**, *51*, 7697–7701; *Angew. Chem.* **2012**, *124*, 7817–7821.

[2] P. Raybaud, H. Toulhoat, *Catalysis by Transition Metal Sulphides, From Molecular Theory to Industrial Application*, Technip, Paris, **2013**.

[3] a) H. Schulz, *Appl. Catal. A* **1999**, *186*, 3–12; b) M. Corral Valero, P. Raybaud, *Catal. Lett.* **2013**, *143*, 1–17.

[4] a) F. Jiao, H. Frei, *Angew. Chem. Int. Ed.* **2009**, *48*, 1841–1844; *Angew. Chem.* **2009**, *121*, 1873–1876; b) B. S. Yeo, A. T. Bell, *J. Am. Chem. Soc.* **2011**, *133*, 5587–5593.

[5] X. Xie, Y. Li, Z. Q. Liu, M. Haruta, W. Shen, *Nature* **2009**, *458*, 746–749.

[6] J. L. Ewbank, L. Kovarik, C. C. Kenvin, C. Sievers, *Green Chem.* **2014**, *16*, 885.

[7] P. Euzen, P. Raybaud, X. Krokidis, H. Toulhoat, J. L. Loarer, J.-P. Jolivet, C. Froidefond, in *Handbook of Porous Solids* (Eds.: F. Schüth, K. S. W. Sing, J. Weitkamp), Wiley-VCH, Weinheim, **2002**.

[8] C. Chizallet, P. Raybaud, *Angew. Chem. Int. Ed.* **2009**, *48*, 2891–2893; *Angew. Chem.* **2009**, *121*, 2935–2937.

[9] A. Jean-Marie, A. Griboval-Constant, A. Y. Khodakov, F. Diehl, *C. R. Chim.* **2009**, *12*, 660–667.

[10] a) J. L. Paulhiac, O. Clause, *J. Am. Chem. Soc.* **1993**, *115*, 11602–11603; b) W. Chu, P. Chernavskii, L. Gengembre, G. Pankina, P. Fongarland, A. Khodakov, *J. Catal.* **2007**, *252*, 215–230; c) A. K. Dalai, B. H. Davis, *Appl. Catal. A* **2008**, *348*, 1–15; d) L. Vandewater, G. Bezemer, J. Bergwerff, M. Versluijshelder, B. Weckhuysen, K. De Jong, *J. Catal.* **2006**, *242*, 287–298; e) P. Munnik, P. E. de Jongh, K. P. de Jong, *J. Am. Chem. Soc.* **2014**, *136*, 7333–7340.

[11] J. Vakros, K. Bourikas, S. Perlepes, C. Kordulis, A. Lycourghiotis, *Langmuir* **2004**, *20*, 10542–10550.

[12] S. N. Towle, J. R. Bargar, G. E. Brown Jr., G. A. Parks, *J. Colloid Interface Sci.* **1997**, *187*, 62–82.

[13] a) A. Gorczyca, V. Moizan, C. Chizallet, O. Proux, W. Del Net, E. Lahera, J. L. Hazemann, P. Raybaud, Y. Joly, *Angew. Chem. Int. Ed.* **2014**, *53*, 12426–12429; *Angew. Chem.* **2014**, *126*, 12634–12637; b) C. Chizallet, P. Raybaud, *Catal. Sci. Technol.* **2014**, *4*, 2797; c) M. J. Louwerse, G. Rothenberg, *ACS Catal.* **2013**, *3*, 1545–1554; d) T. Kropp, J. Paier, J. Sauer, *J. Am. Chem. Soc.* **2014**, *136*, 14616–14625; e) R. A. van Santen, *Angew. Chem. Int. Ed.* **2014**, *53*, 8618–8620; *Angew. Chem.* **2014**, *126*, 8762–8764.

[14] a) F. Averseng, M. Vennat, M. Che, *Handbook of Heterogeneous Catalysis*, Wiley-VCH, Weinheim, **2008**; b) L. Vordonis, N. Spanos, P. G. Koutsoukos, A. Lycourghiotis, *Langmuir* **1992**, *8*, 1736–1743; c) H. Tamura, N. Katayama, R. Furuichi, *J. Colloid Interface Sci.* **1997**, *195*, 192–202.

[15] E. Fischer, *Ber. Dtsch. Chem. Ges.* **1894**, *27*, 2985–2993.

[16] a) J. M. Lehn, *Supramolecular Chemistry, concepts and perspectives*, Wiley-VCH, Weinheim, **1991**; b) S. H. Gellman, *Chem. Rev.* **1997**, *97*, 1231–1232.

[17] S. Boujday, J. F. Lambert, M. Che, *J. Phys. Chem. B* **2003**, *107*, 651–654.

[18] a) M. Digne, P. Sautet, P. Raybaud, P. Euzen, H. Toulhoat, *J. Catal.* **2002**, *211*, 1–5; b) M. Digne, P. Sautet, P. Raybaud, P. Euzen, H. Toulhoat, *J. Catal.* **2004**, *226*, 54–68.

[19] Y. Sakashita, T. Yoneda, *J. Catal.* **1999**, *185*, 487–495.

[20] F. Leydier, C. Chizallet, A. Chaumonnot, M. Digne, E. Soyer, A. A. Quoineaud, D. Costa, P. Raybaud, *J. Catal.* **2011**, *284*, 215–229.

[21] P. Munnik, N. A. Krans, P. E. de Jongh, K. P. de Jong, *ACS Catal.* **2014**, *4*, 3219–3226.

[22] G. Kresse, J. Hafner, *Phys. Rev. B* **1994**, *49*, 14251–14269.

[23] J. Perdew, K. Burke, M. Ernzerhof, *Phys. Rev. Lett.* **1996**, *77*, 3865–3868.

[24] G. Kresse, D. Joubert, *Phys. Rev. B* **1999**, *59*, 1758–1775.

Received: March 4, 2015
Revised: March 25, 2015
Published online: April 23, 2015

